Materials Physics and Mechanics 45 (2020) 8-19 Received: March 11, 2020

# MODELING MICROSTRUCTURE EVOLUTION DURING THERMOMECHANICAL PROCESSING AND HEAT TREATMENT OF STEELS AND PREDICTING THEIR MECHANICAL PROPERTIES

**A.A. Vasilyev[1*], D.F. Sokolov[2], S.F. Sokolov[2]**

[1]Peter the Great St. Petersburg Polytechnic University, Polytekhnicheskaya 29, 195251, St. Petersburg

[2]PJSC Severstal, Mira 30, 162608, Cherepovets, Russian Federation

*e-mail: vasilyev_aa@mail.ru

**Abstract.** An integral computer model/program AusEvol Pro was developed to describe the evolution of steel microstructure during thermomechanical processing (hot rolling, forging), as well as subsequent heat treatment (normalization, tempering), and to evaluate the final mechanical properties (yield stress, tensile stress, elongation), hardness and impact toughness. The program implements a set of physically based models that allow quantitative description of all significant processes of steel structure formation with account of the effects of chemical composition both during thermomechanical processing and heat treatment. Calculations of the final mechanical properties are carried out using the developed models that take into account all physically meaningful contributions. The models created are verified both on the extensive database of our own experimental studies and on reliable data from literature for steels of various chemical compositions.

**Keywords:** heat treatment, mechanical property, microstructure, modeling, steel, thermo-mechanical processing

## 1. Introduction

In the last 30 years considerable attention has been paid to the development of integral quantitative models which enable describing a complex evolution of the microstructure of steels under their thermomechanical processing in industrial hot rolling and subsequent accelerated cooling, as well as predicting the final mechanical properties [1-7]. Such integral models, implemented with computer programs [6,7], are successfully used in the practice of industrial production, allowing to optimize the rolling modes of existing steel grades, as well as to quickly develop new steel grades and their production modes. However, the microstructure of thermomechanically processed steels evolves further during additional heat treatments (normalization or tempering); thus, to develop the physically based models for underlying processes is a task of great practical significance which currently receives considerable attention.

This paper briefly describes the integral computer model/program AusEvol Pro that was developed to predict the evolution of steel microstructure during both the thermomechanical processing and subsequent heat treatment, as well as to evaluate the final mechanical properties (yield stress, tensile stress, elongation), hardness and impact toughness. The resulting final properties of steels after the hot rolling and the latter in combination with subsequent heat treatment, performed in accordance with real industrial conditions, are compared with experimental data.

http://dx.doi.org/10.18720/MPM.4512020_2

## 2. Brief description of the computer model/program AusEvol Pro

The AusEvol Pro computer model is designed to solve the following problems relevant to modern low-alloyed steels:

- simulation of thermomechanical processing according to its specified modes;
- simulation of specific heat treatments;
- calculation of the CCT-diagrams;
- calculation of the TTT-diagrams.

The program with a user-friendly interface was implemented in the C++ language and can work on Microsoft Windows family operating systems.

AusEvol Pro involves previously developed models for the main microstructural phenomena during thermomechanical processing of austenite while allowing for chemical composition of steel:

- grain growth;
- dynamic recrystallization;
- static recrystallization taking into account the effects of recovery and microalloying elements (MAE) (Nb, Ti, V) carbonitride/carbide precipitation on the dislocations of the deformed austenite;
- austenite transformation under continuous cooling with allowance for the effects of accumulated strain on the formation of ferrite and bainites of various morphology;
- recovery of α−phase and precipitations in the latter under cooling of the transformed structure.

Additionally, the model is extended to simulate the evolution of microstructure during subsequent heat treatments:

- austenitization of the complex initial microstructure under its heating and following decomposition in cooling (normalization);
- recovery and precipitation of different carbides ($Fe_3C$, $V_4C_3$, $Mo_2C$, $Cr_7C_3$) and particles of pure Cu during tempering.

Calculations of the final mechanical properties, hardness and impact toughness are carried out using the corresponding models that take into account all physically meaningful contributions. The partial models of AusEvol Pro are briefly described below.

**Grain growth model.** This model [8] assumes proportionality of the austenite grain growth activation energy to the activation energy of bulk self-diffusion ($Q_{SD}$) dependent on chemical composition of solid solution in accordance with a previously obtained formula [9]. The model has been calibrated with the data on the isothermal grain growth kinetics in the temperature range 1000÷1200°C for two industrial (S1(DQSK), S2(A36) [10,11]) and 8 laboratory (S3-S10 [12,13]) steels whose chemical compositions are listed in Table1.

Comparison of predicted to actual grain sizes for all considered steels and temperatures shown in Fig. 1 confirms the model performance; indeed, the average magnitude of relative error does not exceed 11% comparable to measurement errors. The model allows obtaining good agreement with experiment for the considered steels in which the minimum (~ 79.7 kJ/mol) and maximum (~ 243.7 kJ/mol) values of the activation energy of grain growth differ by 3 times (Table 1). The average relative error in calculating grain size is about 11% that is comparable to the measurement error.

Table 1. Chemical compositions (mass.%) of steels used to calibrate the grain growth model. $Q_{GG} = 0.5Q_{SD}$ is the grain growth activation energy provided that all alloying elements are in solid solution (its minimum and maximum values are marked in bold)

| Steel | C | Mn | Si | Ni | Cr | Mo | Nb | Al | N | $Q_{GG}$, kJ/mol | Ref. |
|---|---|---|---|---|---|---|---|---|---|---|---|
| S1 | 0.17 | 0.74 | 0.01 | - | - | - | - | 0.04 | 0.005 | **79.7** | [10,11] |
| S2 | 0.04 | 0.30 | 0.01 | - | - | - | - | 0.04 | 0.005 | 88.7 | |
| S3 | 0.08 | 0.49 | 0.26 | - | - | 0.49 | - | - | - | 197.1 | [12] |
| S4 | 0.21 | 1.47 | 0.27 | - | 1.0 | 0.49 | - | - | - | 183.2 | |
| S5 | 0.32 | 1.01 | 0.29 | - | 2.0 | 0.50 | - | - | - | 161.2 | |
| S6 | 0.09 | 0.95 | 0.27 | 2.0 | 1.0 | 0.50 | - | - | - | 180.8 | |
| S7 | 0.19 | 0.52 | 0.27 | 2.0 | 2.0 | 0.49 | - | - | - | 153.2 | |
| S8 | 0.20 | 1.04 | 0.26 | 4.0 | - | 0.49 | - | - | - | 154.5 | |
| S9 | 0.32 | 1.51 | 0.27 | 2.0 | - | 0.50 | - | - | - | 146.1 | |
| S10 | 0.05 | 1.88 | 0.04 | - | - | 0.49 | 0.048 | 0.05 | 0.004 | **243.7** | [13] |

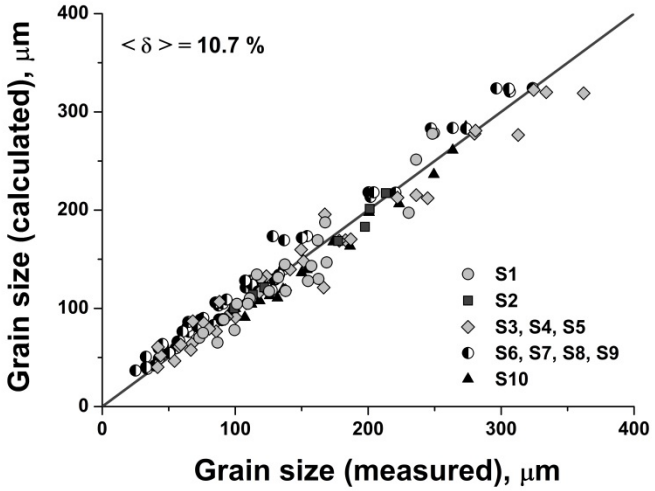


**Fig. 1.** Comparison of model predictions to actual austenite grain sizes; <δ> is the magnitude of an average relative error

**Recrystallization model.** The model for austenite dynamic recrystallization [3], very close to the model of S.F. Medina [14], has been fitted to the data set obtained on 18 microalloyed (Nb, Ti, and V) steels with different amounts of C, Mn, Si, Mo. The proposed model employs a generalized expression for the characteristic threshold strain based on numerous data for 18 above-mentioned steels and, additionally, for microalloyed line-pipe steels [3].

A physically based model, developed to describe the kinetics of austenite static recrystallization, allows predict the recrystallized grain size, its dependence on temperature, parameters of deformation and the chemical composition of low-alloyed steels [15]. This model actually takes in account the three mutually interacting processes: recrystallization, recovery and precipitation of carbonitrides/carbides of MAE (Nb(C,N), V(C,N), TiC) on the dislocations in deformed austenite. As in the case of the grain growth model, it is assumed that the activation energy of lattice reconstruction during recrystallization is proportional to the activation energy of bulk self-diffusion; the latter significantly depends, according to [9], on the chemical composition of solid solution.

To simulate simultaneously the three interrelated processes (recovery, recrystallization, deformation-induced precipitation), empirical parameters of the model have been determined in two steps. First, the recrystallization parameters, allowing for the concurrent recovery, are found while assuming that the atoms of all alloying elements, including MAE, are completely dissolved in the austenite, i.e. no precipitation takes place. Next, additional parameters, needful for modeling the precipitation kinetics and the interaction of nascent particles with the boundaries of recrystallized grains, are obtained. All the parameters are fitted to the wide experimental data on austenite recrystallization for 21 steels with a wide range of chemical composition listed in Table 2.

Table 2. Chemical composition (mass.%) of steels employed in model calibration

| Steel | C | Mn | Si | Cr | Ni | Mo | Nb | V | Ti | N | Ref. |
|---|---|---|---|---|---|---|---|---|---|---|---|
| S1 | 0.11 | 0.55 | 0.26 | - | - | - | - | - | - | - | [16-21] |
| S2 | 0.53 | 0.71 | 0.21 | - | - | - | - | - | - | - | |
| S3 | 0.42 | 0.79 | 0.27 | - | - | 0.18 | - | - | - | - | |
| S4 | 0.44 | 0.79 | 0.23 | - | - | 0.38 | - | - | - | - | |
| S5 | 0.11 | 1.32 | 0.24 | - | - | - | 0.070 | - | - | - | |
| S6 | 0.12 | 1.10 | 0.24 | - | - | - | - | 0.07 | - | - | |
| S7 | 0.15 | 1.25 | 0.27 | - | - | - | - | - | 0.017 | - | |
| S8 | 0.08 | 1.47 | 0.20 | - | - | 0.19 | 0.042 | 0.06 | 0.010 | 0.006 | Own results |
| S9 | 0.04 | 1.90 | 0.25 | 0.11 | 0.45 | 0.31 | 0.051 | 0.02 | 0.020 | 0.005 | |
| S10 | 0.11 | 0.36 | 0.23 | 0.39 | 1.91 | 0.31 | 0.011 | 0.01 | - | - | |
| S11 | 0.11 | 1.23 | 0.24 | - | - | - | 0.041 | - | - | 0.0112 | [16-21] |
| S12 | 0.11 | 1.32 | 0.24 | - | - | - | 0.093 | - | - | 0.0119 | |
| S13 | 0.21 | 1.08 | 0.18 | - | - | - | 0.024 | - | - | 0.0058 | |
| S14 | 0.21 | 1.14 | 0.19 | - | - | - | 0.058 | - | - | 0.0061 | |
| S15 | 0.11 | 1.10 | 0.24 | - | - | - | - | 0.043 | - | 0.0105 | |
| S16 | 0.12 | 1.10 | 0.24 | - | - | - | - | 0.060 | - | 0.0123 | |
| S17 | 0.11 | 1.05 | 0.24 | - | - | - | - | 0.093 | - | 0.0144 | |
| S18 | 0.21 | 1.10 | 0.20 | - | - | - | - | 0.062 | - | 0.0134 | |
| S19 | 0.15 | 1.25 | 0.27 | - | - | - | - | - | 0.055<br>**0.021*** | - | |
| S20 | 0.15 | 1.10 | 0.26 | - | - | - | - | - | 0.075<br>**0.040*** | - | |
| S21 | 0.06 | 1.70 | 0.20 | - | - | 0.20 | 0.045 | 0.040 | 0.020 | 0.005 | Own results |

*Contents obtained by taking into account Ti binding in TiN particles

Figure 2 demonstrates good prediction power of the model for the kinetics of austenite recrystallization in steels S1-S10 with allowance for recovery in a wide range of temperature, initial grain size and deformation conditions. The average relative error of the predicted recrystallized fractions does not exceed 13%.

Figure 3 illustrates the correspondence of modeling results to the experimental data on recrystallization kinetics in various micro-alloyed steels with account of the precipitation of carbonitrides/carbides of MAE (Nb(C,N), V(C,N), TiC) on the dislocations in deformed austenite. Apparently, the model has good performance in application to both steels micro-alloyed by one of Nb, V, Ti (Fig. 3a,b; 3c,d, and 3e, respectively) and the complexly micro-alloyed steels (Fig. 3f).

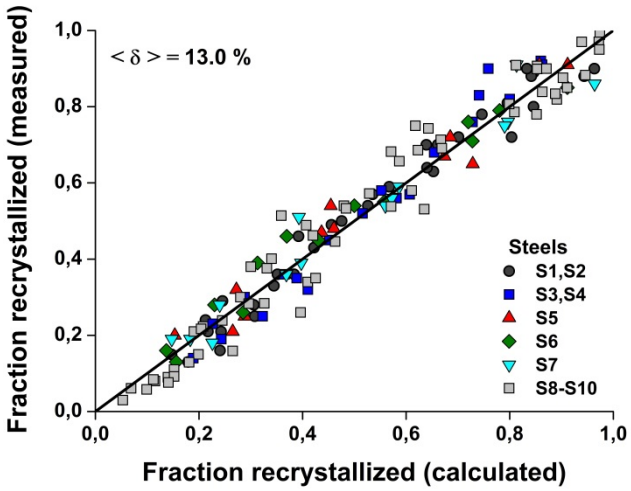


**Fig. 2.** Comparison of model predictions to actual recrystallized fractions for steels S1-S10; <δ> is the magnitude of an average relative error

The proposed model of austenite recrystallization complies well with the experiments on numerous steels in a wide range of temperature (825÷1200ºC), initial grain size (30÷285 μm), the degree (0.2÷0.35) and rate (0.5÷5 $s^{-1}$) of strain. The process activation energy in the considered wide range of chemical compositions varies by more than two times (146.1 to 308.1 kJ/mol).

**Austenite transformation model.** The physically based models of the ferritic and pearlitic transformations are described in detail elsewhere [22]. Our approach to the ferritic transformation differs from the existing analogues by the novel formulation of complex alloying effect on the nucleation rate of ferrite grains and mobility of α/γ–boundaries. Moreover, the model takes into account the effect of alloying by substitutional elements on the carbon diffusion coefficient in bulk austenite [23]. The bainitic transformation model is briefly described in [4].

The empirical parameters for the employed partial models were determined on the ground of our extensive database on the austenite transformation kinetics for 39 steels with a wide range of chemical composition (C(0.004÷0.74); Mn(0.14÷1.90); Si(0.01÷1.58); Cr(0.01÷1.08); Ni(0.01÷3.50); Cu(0.01÷1.10); Mo(0.003÷0.52); Nb(0.002÷0.056); V(0.002÷0.124); Ti(0.001÷0.08) (mass.%)), as well as on the ferrite grain sizes for some of them. The cooling rate and austenite grain size were varied in a wide range (cooling rate: 1÷200°C/s; austenite grain size: 20÷130 μm) to obtain the spectrum of practically important microstructures.

A phenomenological model of martensitic transformation is based on a database on its kinetics compiled for 14 steels with chemical compositions varying over a wide range (C(0.04÷0.74), Mn(0.35÷1.64), Si(0.20÷1.58), Cr(0.04÷1.08), Ni(0.04÷3.50), Mo(0.01÷0.52) (mass.%)), as well as on the measurements of initial austenite grain size. As a result, a satisfactorily accurate empirical formula was obtained for the martensite start temperature $M_S$:

$$M_S(°C) = \left(554 - 394w_C - 36w_{Mn} - 15w_{si} - 35w_{Cr} - 16w_{Ni} - 8.5w_{Mo}\right)\left(1 - \exp\left(-D_\gamma^{0.5}\right)\right),$$

where $w_C, w_{Mn}, w_{si}, w_{Cr}, w_{Ni}, w_{Mo}$ are the quantities (mass.%) of the corresponding alloying elements; $D_\gamma$ is the average volumetric size of an austenite grain (μm).

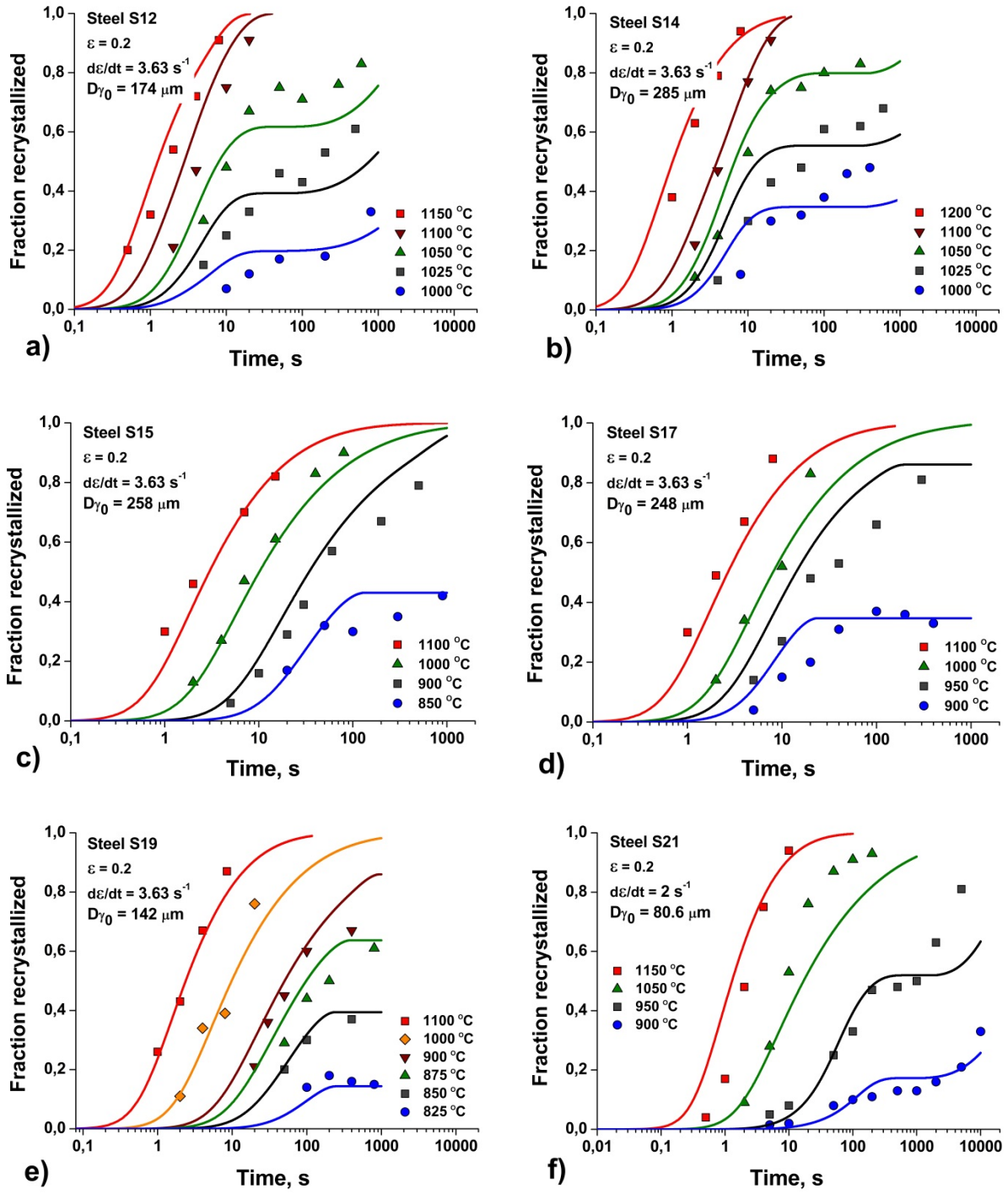


**Fig. 3.** Comparison of modeling the recrystallization kinetic curves for various micro-alloyed steels, with account of precipitation of carbonitrides/carbides at different temperatures, sizes of the initial austenite grains ($D_{\gamma 0}$) and deformation parameters (ε, dε/dt), with experimental data (symbols)

The developed model makes it possible to describe with good accuracy the austenite transformation in low alloyed steels under continuous cooling with the formation of all practically important structural components (ferrite, pearlite, bainites of different morphology and martensite) taking into account the effects of chemical composition, as well as the effect of austenite pre-deformation.

**Austenitization model.** The model [24] has been developed to describe the kinetics of austenitization for steels with complex microstructure under continuous heating and to predict austenite grain size in dependence on chemical composition, volume fractions of the structural components (ferrite, pearlite, bainite, martensite), ferrite grain size and heating rate. The empirical parameters were defined on the base of own kinetics data for austenitization under continuous heating at rates of 0.5, 1, 3, 10, 50°C/s for various complex microstructures of 8 industrial steel grades with a wide range of chemical compositions (Table 3).

The calculated austenitization curves for a number of studied steels with different mixed initial microstructures including polygonal ferrite (PF), pearlite (P), bainite (B) and martensite (M) together with experimental data are presented in Fig. 4. As one can see, the developed model accurately reproduces the process kinetics in a wide range of heating rates. Average absolute value of relative error in calculating the austenitization curves is equal to 9.4%. The predicted values of austenite grain size are also in a good agreement with the experimental data (Fig. 5). Note, that the average absolute value of relative error in calculating the grain size does not exceed 17.5%, which is comparable with the corresponding error of its measurements.

Table 3. Chemical compositions of the investigated steels (mass.%)

| Steel | C | Mn | Si | Cr | Ni | Cu | Mo | Nb | V | Ti |
|---|---|---|---|---|---|---|---|---|---|---|
| 45Х * | 0.45 | 0.68 | 0.31 | 0.96 | 0.06 | 0.12 | 0.01 | 0.003 | 0.004 | 0.003 |
| 65Г * | 0.66 | 0.95 | 0.33 | 0.10 | 0.09 | 0.11 | 0.01 | 0.002 | 0.002 | 0.002 |
| 12Х1МФ * | 0.13 | 0.56 | 0.20 | 0.94 | 0.21 | 0.13 | 0.26 | 0.002 | 0.152 | 0.002 |
| 13ХФА * | 0.12 | 0.44 | 0.23 | 0.61 | 0.07 | 0.12 | 0.02 | 0.024 | 0.054 | 0.003 |
| АБ2 * | 0.08 | 0.37 | 0.25 | 0.41 | 1.94 | 0.52 | 0.25 | 0.002 | 0.031 | 0.003 |
| 18ХГНМФР * | 0.20 | 1.47 | 0.30 | 0.85 | 1.49 | 0.28 | 0.28 | 0.041 | 0.124 | 0.063 |
| 14ХГ2САФД * | 0.17 | 1.55 | 0.56 | 0.64 | 0.26 | 0.14 | 0.03 | 0.002 | 0.051 | 0.002 |
| S690 | 0.12 | 0.97 | 0.30 | 1.08 | 0.24 | 0.17 | 0.52 | 0.033 | 0.006 | 0.003 |

* Russian steel grades

**Tempering model.** The model has been developed for describing the evolution of the microstructure of quenched steels during subsequent tempering as a result of recovery and precipitation of different carbides ($Fe_3C$, $V_4C_3$, $Mo_2C$, $Cr_7C_3$) and pure Cu particles in the α−phase of the bainitic-martensitic quenching structures. The recovery kinetics is calculated according to [25]. The calculations of thermodynamic driving forces for precipitation of various carbides and particles of pure copper, as well as the equilibrium concentrations of alloying elements in the solid solution, were made using Thermo-Calc package [26]. The volume diffusion coefficients of atoms of alloying elements in ferrite are taken from the literature [27,28]. At the same time, an original formula is used for calculating the carbon diffusion coefficient in alloyed ferrite [23,29], which takes into account the effect of the substitution alloying element contents (Mn, Ni, Cr, Mo, Si).

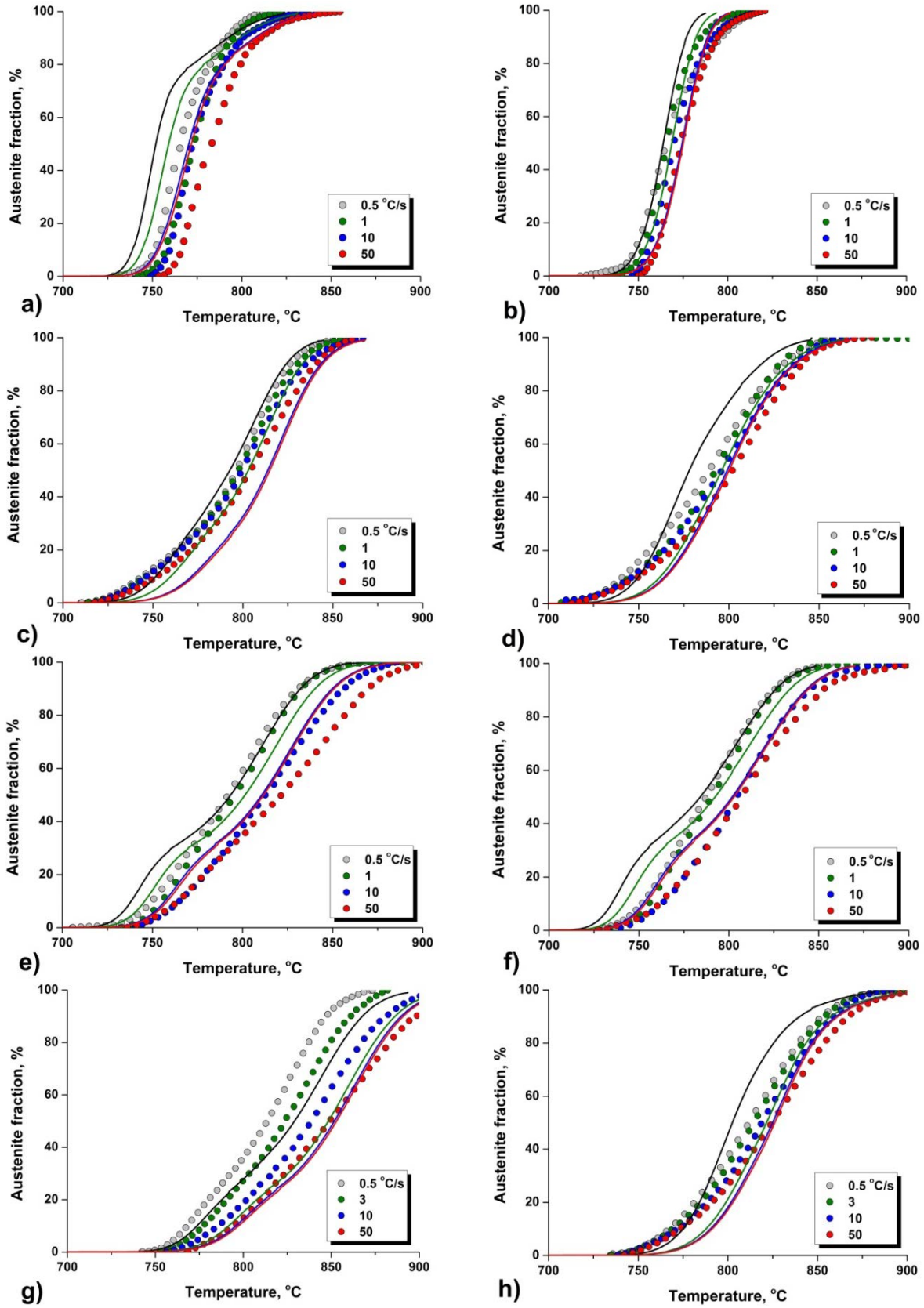


**Fig. 4.** Calculated austenitization curves for different heating rates of a number of investigated steels with different predicted microstructures in comparison with experimental data (symbols). **45Х:** PF + PE (a), M (b); **АБ2:** PF + PE + B (c), PF + B (d); **14ХГ2САФД:** PF + PE + B (e), PF + B + M (f); **S690:** PF + PE (g), PF + B (h)

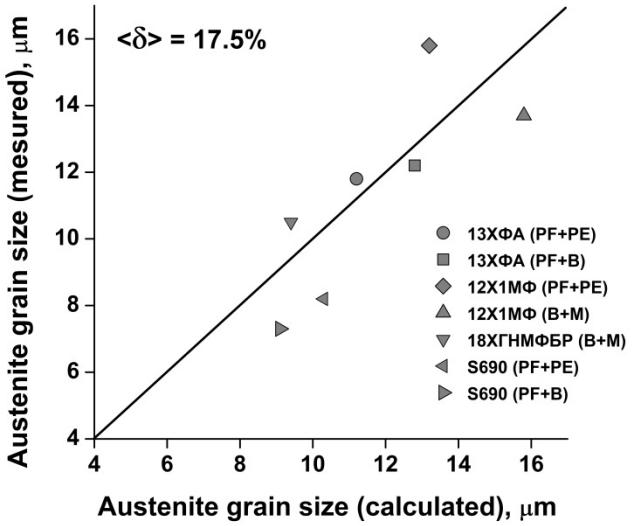


**Fig. 5.** Comparison of the calculated and measured austenite grain sizes for various steels; <δ> is the average absolute value of the relative error of calculations

**Mechanical properties model.** The model is aimed to predict the mechanical properties of bainitic-martensitic structures of steels formed by quenching, as well as subsequent tempering. To verify the model, we used the data on mechanical properties (yield strength, tensile strength, elongation), as well as hardness and impact toughness, for 10 industrial quenched steels of the bainitic-martensitic class with a wide range of chemical composition ((C(0.04÷0.27); Mn(0.33÷1.57); Si(0.22÷1.09); Cr(0.02÷1.14); Ni(0.01÷3.74); Cu(0.02÷1.03); Mo(0.001÷0.43); Nb(0.002÷0.044); V(0.003÷0.20); Ti(0.001÷0.045); B(0.0003÷0.0032) (mass.%)), that underwent tempering at different temperatures.

The characteristics (volume densities and average dimensions) of dispersed particles formed during steel tempering, dislocation density, and the concentration of alloying elements in the solid solution, depending on the tempering time at different temperatures, were calculated with the developed structural model of tempering. The model is eventually calibrated using the obtained sets of experimental and calculated data.

*The main advantage of the listed models for describing the steel structure formation is in physically justified effects of all practically important alloying elements. This advantage enables efficient use of AusEvol Pro program for a large number of steel grades with a wide range of chemical composition.*

## 3. Predicted mechanical properties of steels processed at different industrial conditions

The final mechanical properties of industrial steels were calculated for 160 modes of industrial processing, which include 22 modes of hot rolling (HR), 49 modes of processing according to the scheme hot rolling + normalization (HR + N), 7 modes of hot rolling + hardening (HR + Q) and 83 modes hot rolling + hardening + tempering (HR + Q + T). The ranges of chemical compositions of the considered steels are shown in Table 4. Figure 6 represents actual final properties of steels calculated with the AusEvol Pro model to evaluate the prediction accuracy.

Table 4. Range of chemical compositions of steels subjected to various technological treatments (HR, HR + N, HR + Q, HR + Q + T)

| | Chemical composition (mass.%) | | | | | | | | | | | |
|---|---|---|---|---|---|---|---|---|---|---|---|---|
| | | C | Mn | Si | Cu | Ni | Mo | Cr | Nb | V | Ti | B |
| HR | min | 0.08 | 0.42 | 0.02 | 0.03 | 0.02 | 0.002 | 0.03 | 0.001 | 0.002 | 0.002 | - |
| | max | 0.19 | 1.63 | 0.29 | 0.20 | 0.24 | 0.016 | 0.84 | 0.044 | 0.073 | 0.016 | - |
| HR + N | min | 0.11 | 0.41 | 0.17 | 0.04 | 0.02 | 0.002 | 0.03 | 0.001 | 0.002 | 0.001 | 0 |
| | max | 0.66 | 1.64 | 0.78 | 0.40 | 0.54 | 0.058 | 0.86 | 0.050 | 0.068 | 0.017 | 0.001 |
| HR + Q | min | 0.27 | 0.57 | 1.07 | 0.07 | 1.41 | 0.230 | 0.84 | 0.022 | 0.004 | 0.067 | 0.003 |
| | max | | | | | | | | | | | |
| HR + Q + T | min | 0.06 | 0.33 | 0.18 | 0.03 | 0.02 | 0.002 | 0.03 | 0.001 | 0.002 | 0.002 | 0 |
| | max | 0.27 | 1.65 | 1.10 | 0.55 | 1.99 | 0.410 | 1.14 | 0.045 | 0.100 | 0.050 | 0.003 |

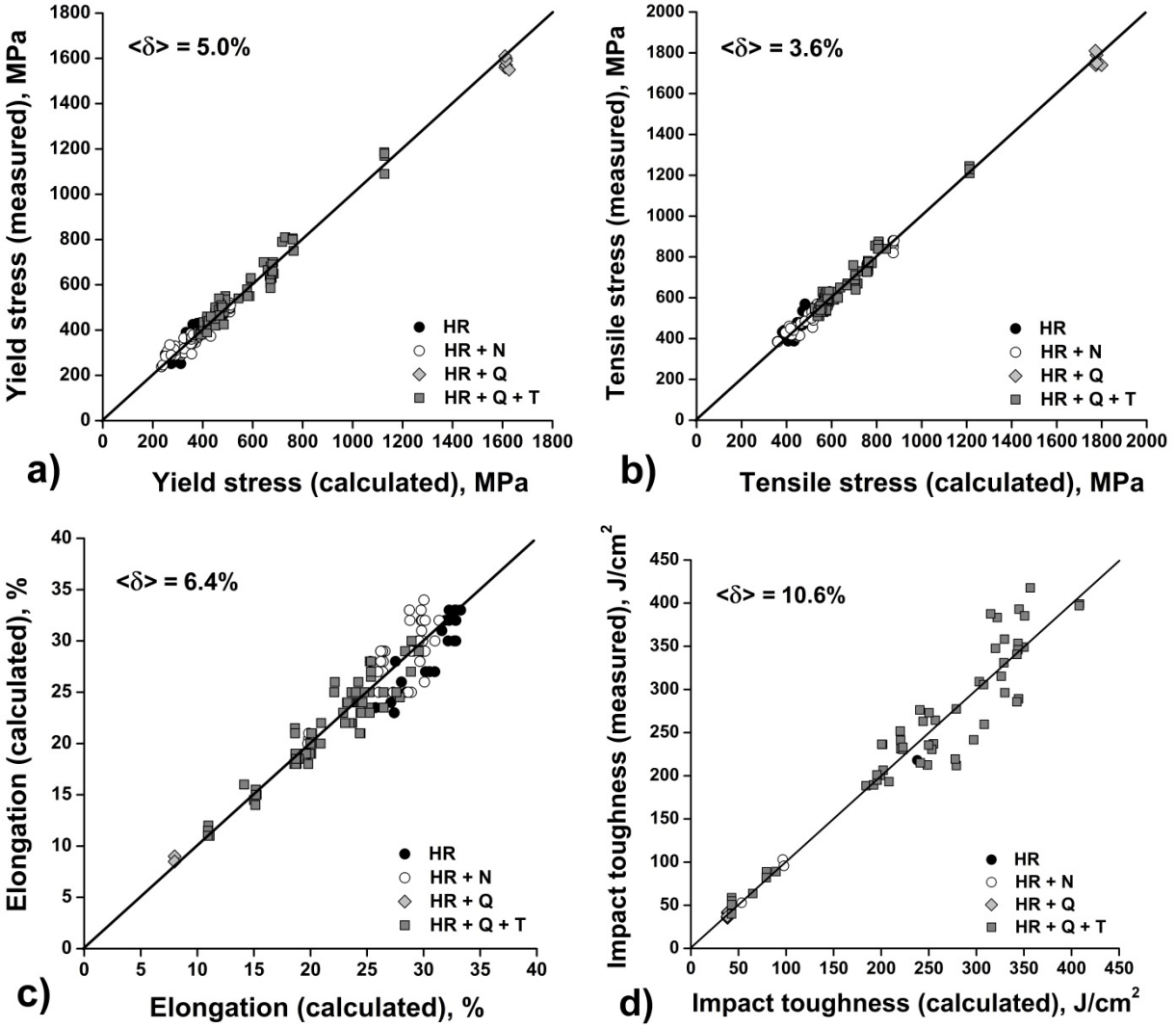


**Fig. 6.** Comparison of the calculated and measured final properties of the investigated steels. a) yield stress; b) tensile stress; c) elongation; d) impact toughness. <δ> is a relative error

## 4. Conclusions

The integral computer model/program AusEvol Pro was developed to predict the evolution of steel microstructure during thermomechanical processing (hot rolling, forging), as well as subsequent heat treatment (normalization, tempering), and to evaluate the final mechanical

properties (yield stress, tensile stress, elongation), hardness and impact toughness. Complex alloying effects are quantified on both the austenite structure evolution (grain growth, recrystallization, carbides precipitation) in hot deformation and the phase transformation in cooling. The final steel properties are treated in terms of volume fractions of main structure constituents with various individual properties. Good correspondence of the predictions to relevant experimental data confirms performance of the model in the development and improvement of industrial technologies of steel production.

***Acknowledgments.*** *This work was supported by the grant from the Russian Science Foundation (project No. 19-19-00281).*

**References**

[1] Andorfer J, Auzinger D, Buchmayr B, Giselbrecht W, Hriberning G, Hubmer G, Luger A, Samoilov A. Prediction of the as hot rolled properties of plain carbon steels and HSLA steels. *BHM*. 1997;142: 374-377.

[2] Militzer M, Howbolt EB, Meadowcroft TR. Microstructural model for hot strip rolling of high-strength low-alloy steels. *Metallurgical and Materials Transactions A.* 2000;32: 1247-1259.

[3] Vasilyev A, Rudskoy A, Kolbasnikov N, Sokolov S, Sokolov D. Physical and mathematical modeling of austenite microstructure evolution processes developing in line-pipe steels under hot rolling. *Material Science Forum*. 2012;706-709: 2836-2841.

[4] Sokolov D, Ogoltcov A, Vasilyev A, Kolbasnikov N, Sokolov S. Modeling of microstructure and mechanical properties of hot rolled steels. *Material Science Forum*. 2013;762: 116-121.

[5] Sokolov D, Vasilyev A, Ogoltcov A, Sokolov S, Kolbasnikov N. Modeling mechanical properties of steels with complex microstructure. In: *METAL 2014 Conference Proceedings*. 2014. p.482-487.

[6] Ogoltcov A, Sokolov D, Sokolov S, Vasilyev A. STAN 2000: Computer model for simulation of steels hot rolling on mill 2000 of Severstal. In: *METAL 2015 Conference Proceedings*. 2015. p.221-226.

[7] Ogoltcov A, Sokolov D, Sokolov S, Vasilyev A. Computer model STAN 2000 and its use in practice of steels hot rolling on mill 2000 of Severstal. *Material Science Forum*. 2016;854: 183-189.

[8] Vasilyev AA, Sokolov SF, Sokolov DF, Kolbasnikov NG. Modeling of grain growth kinetics in complexly alloyed austenite. *Letters on Materials*. 2019;9(4): 419-423.

[9] Vasilyev A, Sokolov S, Kolbasnikov N, Sokolov D. Effect of alloying on the self-diffusion activation energy in γ-iron. *Physics of the Solid State*. 2011;53: 2194-2200.

[10] Militzer M, Meadowcroft TR, Hawbolt EB, Giumelli A. Austenite grain growth kinetics in Al-killed plain carbon steels. *Metallurgical and Materials Transactions A.* 1996;27: 3399-3409.

[11] Giumelli AK, Militzer M, Hawbolt EB. Analysis of the austenite grain size distribution in plain carbon steels. *Iron and Steel Institute of Japan International*. 1999;39(3): 271-280.

[12] Uhm S, Moon J, Lee C, Yoon J, Lee B. Prediction model for the austenite grain size in the coarse grained heat affected zone of Fe-C-Mn steels: Considering the effect of initial grain size on isothermal growth behavior. *Iron and Steel Institute of Japan International*. 2004;44(7): 1230-1237.

[13] Sarkar S, Moreau A, Militzer M, Poole WJ. Evolution of austenite recrystallization and grain growth using laser ultrasonics. *Metallurgical and Materials Transactions A*. 2008;39(4): 897-907.

[14] Medina SF, Hernandez CA. Modeling of the dynamic recrystallisation of austenite in low alloy and microalloyed steels. *Acta Materialia*. 1996;44(1): 165-171.
[15] Vasilyev AA, Sokolov SF, Sokolov DF, Kolbasnikov NG. Modeling of static recrystallization in complexly alloyed austenite. *Materials Physics and Mechanics*. 2020;44(3): 229-237.
[16] Medina SF, Mancilla JE, Hernandez CA. Static recrystallization of hot deformed austenite and induced precipitation kinetics in vanadium micro-alloyed steels. *Iron and Steel Institute of Japan International*. 1994;34(8): 689-696.
[17] Medina SF, Mancilla JE. Influence of alloying elements in solution on static recrystallization kinetics of hot deformed steels. *Iron and Steel Institute of Japan International*. 1996;36(8): 1063-1069.
[18] Medina SF, Mancilla JE. Static recrystallization modelling of hot deformed steels containing several alloying elements. *Iron and Steel Institute of Japan International*. 1996;36(8): 1070-1076.
[19] Medina SF, Quispe A. Influence of strain on induced precipitation kinetics in micro-alloyed steels. *Iron and Steel Institute of Japan International*. 1996;36(10): 1295-1300.
[20] Quispe A, Medina SF, Valles P. Recrystallization-induced precipitation interaction in a medium carbon vanadium micro-alloyed steel. *Iron and Steel Institute of Japan International*. 1997;37(8): 783-788.
[21] Medina SF, Quispe A, Valles P, Banos JL. Recrystallization-precipitation interaction study of two medium carbon niobium micro-alloyed steels. *Iron and Steel Institute of Japan International*. 1999;39(9): 913-922.
[22] Vasilyev A, Sokolov D, Kolbasnikov N, Sokolov S. Modeling of the $\gamma \rightarrow \alpha$ transformation in steels. *Physics of the Solid State*. 2012;54: 1669-1680.
[23] Vasilyev AA, Golikov PA. *Models for Calculating Carbon Diffusion Coefficient in Steels and Examples of their Practical Use*. St. Petersburg: POLYTECH-PRESS; 2019. (In Russian)
[24] Vasilyev A, Sokolov D, Sokolov S, Rudskoy A. Investigation and modeling the austenitization kinetics of steels with complex microstructure under continuous heating. *Materials Physics and Mechanics*. 2019;42(4): 423-435.
[25] Vasilyev AA, Sokolov SF, Golubkov NA, Zisman AA, Sokolov DF, Rudskoy AI. Artifacts of stress relaxation technique to fit recovery activation parameters for low carbon steels. *Materials Physics and Mechanics*. 2019;42(2): 183-190.
[26] Thermo-Calc Software. Available from: http: //www.thermocalc.com [Accessed 14th October 2020].
[27] Yamasaki S. *Modelling precipitation of carbides in martensitic steels. PhD thesis*. University of Cambridge; 2004.
[28] Christien F, Barbu A. Modelling of copper precipitation in iron during thermal aging and irradiation. *Journal of Nuclear Materials*. 2004;324(2-3): 90-96.
[29] Vasilyev A, Golikov P. Carbon diffusion coefficient in alloyed ferrite. *Materials Physics and Mechanics*. 2018;39(1): 111-119.